Article

Design Requirements for Personal Mobility Vehicle (PMV) with Inward Tilt Mechanism to Minimize Steering Disturbances Caused by Uneven Road Surface

Tetsunori Haraguchi [1,2,*] and Tetsuya Kaneko [3]

[1] Institutes of Innovation for Future Society, Nagoya University, Furocho, Chikusaku, Nagoya 464-8603, Japan
[2] College of Industrial Technology, Nihon University, 1-2-1 Izumi-cho, Narashino 275-8575, Japan
[3] Department of Mechanical Engineering for Transportation, Faculty of Engineering, Osaka Sangyo University, 3-1-1 Nakagaito, Daito 574-8530, Japan; kaneko@ge.osaka-sandai.ac.jp (T.K.)
* Correspondence: haraguchi@nagoya-u.jp (T.H.)

Abstract: Personal Mobility Vehicle (PMV) which has an inward tilting angle turns with the lateral force due to large camber angle, so it is necessary to consider the lateral movement of the tire vertical load axis during turning. Although the steering torque mechanism are very different from those of automobiles, there are not many examples which studied the steering torque mechanism of PMV. In this paper, based on the effects of six components force acting on the tires, a method for setting the steering axis specifications is derived, including the geometrical minimization of steering moment disturbance due to the vertical load reaction force during turning. Although, automobile tires have a significant ground camber angle when traveling on rutted roads, they do not have it on slant roads because the vehicle body tilts along the road surface. On the other hand, in PMV, the vehicle body always keeps upright when traveling both on slanted roads and on rutted roads. Therefore, the tires have ground camber angles on both types of road surface. We study the straight running ability under such road surface disturbances based on the geometrical minimization of steering moment disturbance due to the vertical load reaction force during turning. This straight running ability can be a remarkable strong point of PMV with an inward tilt mechanism.

Keywords: personal mobility vehicle; active tilting; steering axis; steering disturbance; load reaction force; slanted road; rutted road

1. Introduction

Looking back, at the beginning of the 20th century, in the early days of automobiles, there were already proposals for ultra-compact, low-cost mobility aimed at making it affordable for ordinary people. Even after World War II, there were proposals for ultra-compact, low-cost mobility, mainly in the defeated countries of Japan, Germany, and Italy. It was a dream target for aircraft engineers because the development of aircraft was not permitted in the defeated countries. At the same time, it can be said that the aim was to make it affordable for the citizens of the defeated nations, who could not afford large passenger cars, like those from the United States, due to their limited land and economic power.

Both of these first and second generations have in common that the top priority was to obtain the capability of movement at a low cost, while compromising on the performance and satisfaction of ownership as a car. However, as the price of normal-sized cars fell and they became affordable for ordinary people, both generations of ultra-compact mobility were weeded out of the market, ending their product life.

Although, the use of automobiles has improved people's life with the progress of motorization after World War II, the rapid increase in the number of vehicles owned may reduce their convenience due to traffic congestion and lack of parking spaces in urban

 doi:10.20944/preprints202212.0034.v1

areas. In addition, since substantially all automobiles use fossil fuels as their energy source, in recent years it has been pointed out that the CO2 emitted by automobiles contributes significantly to global warming, following home life and the manufacturing industry.

In such a social situation, a new ultra-compact mobility concept called a personal mobility vehicle (PMV) is currently attracting attention. Among them, in recent years, aiming to save space compared to the first and second generations, a new concept with a fairly narrow width has been proposed [1-4]. The difference of the 3rd generation ultra-compact mobility comparing with the 1st and 2nd generations is not that it is inexpensive, but rather that it is "Fun to drive" due to the inward leaning vehicle dynamics and runs with an electric motor. It will be a proposal of a future-oriented new mobility concept.

In this way, PMV is a promising concept for a sustainable mobility society, but compared to automobiles and motorcycles, there are still few examples of research on PMVs. The authors have been continuously conducting research on social acceptability and motion characteristics [3-14], mainly on PMVs with two front wheels and one rear wheel, which actively give an inward tilt angle according to the steering angle and the vehicle speed. In the References [5,6] the energy balance of the active inward-tilting mechanism was discussed as a basic study prior to commercialization of the vehicle. Next, in the References [6-11], obstacle avoidance ability and inner wheel lift phenomenon during sudden steering were discussed as the points related to vehicle stability. In addition, in the References [12-14], as basic characteristics of vehicle dynamics, we have discussed the steady state characteristics peculiar to PMVs that tilt inward when turning, the optimization of the gradient and hysteresis of steering torque characteristics, and the way to predict the turning limit.

When ultra-compact and lightweight vehicles run in general traffic, they face more safety risks than automobiles, just like motorcycles. As described in the Reference [9] regarding obstacle avoidance ability, it can be expected to be safer than automobiles in terms of active maneuverability on good road surfaces. However, from the crash safety point of view, we don't have a good answer yet. Furthermore, research on stability against disturbances such as road surfaces and crosswinds has not progressed sufficiently.

Therefore, in this report, we consider the vehicle's susceptibility to external disturbances input from the road surface, such as sudden changes in load reaction force (impact from the road surface) due to uneven road surfaces, and the inclination of the road surface in the transverse direction such as road slant and ruts. Then the design requirements for the steering axis of the PMVs, which the authors have been studying, are derived in order to maintain straight-line stability against such disturbances. This report is a technical guideline for realizing such ultra-compact PMVs.

2. Vehicle and Tire Specifications

The object of this report is a PMV with an inward-tilting mechanism with two front wheels and one rear wheel. The static dimensional and mass specifications in Figure 1 and Table 1 are the basic information for Chapter 4.,5.,6. However, in Chapter 4.,5.,6., we will try to optimize the design specifications as a general solution mainly from the static mechanical equilibrium conditions, so we do not need all the dimensions and mass specifications in the discussion. Unless otherwise noted in Chapter 4.,5.,6., the inward tilting mechanism does not matter whether it is passive or active. In the explanation of the previous study example in Chapter 4., note that an active inward tilting mechanism is assumed in which the vehicle tilting angle follows the target tilting angle (Equation (1)) that is uniquely determined according to the vehicle speed and steering angle (target tracking control). The inertias in Table 1 will be used in future simulation experiments with multibody dynamics (MBD) models. This MBD model also will incorporates an active inward tilting mechanism.

$$TRA = A\tan^{-1}\left(\frac{\sin(\delta)v^2}{lg}\right) \quad (1)$$

Preprints (www.preprints.org) | NOT PEER-REVIEWED | Posted: 2 December 2022 doi:10.20944/preprints202212.0034.v1

TRA: target roll angle
A: user amplification factor
δ: tire steered angle
v: vehicle speed
l: wheel base

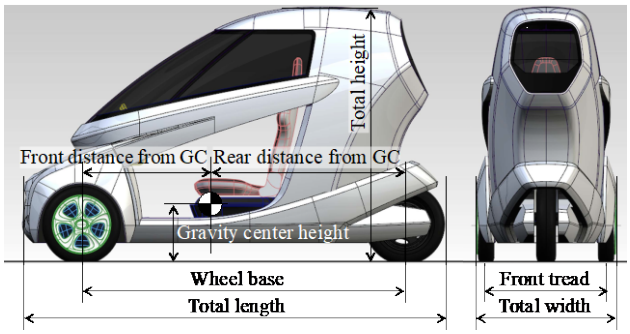

Figure 1. Dimensions of model vehicle [6].

Table 1. Specifications of model vehicle [6].

item	unit	value	item	unit	value
Total length	m	2.645	Total mass	kg	369.8
Total width	m	0.880	Front mass distribution	kg	222.1
Total height	m	1.445	Rear mass distribution	kg	147.7
Wheel base	m	2.020	Roll moment of inertia	kgm^2	58.8
Front distance from gravity center	m	0.807	(Roll moment of inertia of sprung mass)	kgm^2	43.0
Rear distance from gravity center	m	1.213	Pitch moment of inertia	kgm^2	197.3
Front tread	m	0.850	(Pitch moment of inertia of sprung mass)	kgm^2	118.0
Gravity center height	m	0.358	Yaw moment of inertia	kgm^2	187.3
Steering gear ratio	-	16.0	(Yaw moment of inertia of sprung mass)	kgm^2	102.3

The specifications of the 100/90ZR12 size motorcycle tires used in this report are shown in Figure 2, Figure 3, Table 2, which are same as the References [4-15]. The treads of motorcycle tires are characterized by a substantially circular cross-section compared to automobile tires, because they are used with a large camber angle. The cross-sectional shape in Figure 2 corresponds to the value when the tire is properly inflated and no load is applied, and these dimensional specifications become indispensable when considering the lateral movement of the tire contact point when the vehicle is tilted inward in Section 5.2. and Chapter 6. For the sake of simplicity, this report does not consider the elastic deformation of the tire in each direction. Motorcycle tires do not deform much even when under load, therefore when deriving the steering axis specifications from the viewpoint of geometric vehicle mechanisms, it is assumed that there is no error using tire dimensions under no load. The tire characteristic map in Figure 3 is used in Section 4.1. and will be used in the future dynamic simulation. The tire characteristic coefficients in Table 2 are used in the discussion of static balance in Chapter 4.,5.,6., however, like the dimensional and mass specifications of the vehicle, we do not need all coefficients in the discussion of this report.

Preprints (www.preprints.org) | NOT PEER-REVIEWED | Posted: 2 December 2022 doi:10.20944/preprints202212.0034.v1

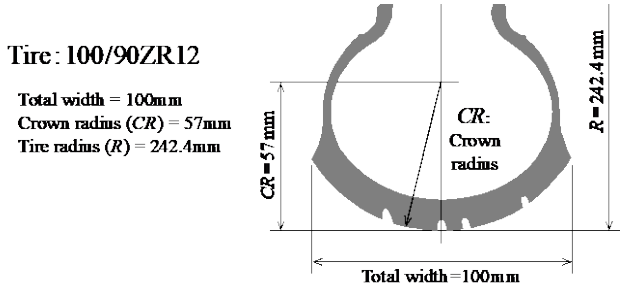

Figure 2. Typical tire cross section (Motorcycle, PMV) [15].

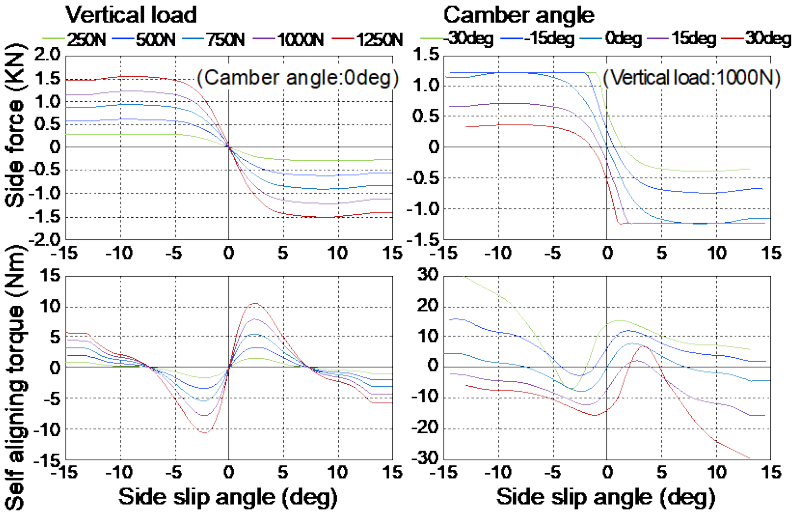

Figure 3. Motorcycle tire model is used in CarMaker [13].

Table 2. Parameters of Tire (100/90R12), Vertical load: F_z=1000N

item	value	item	value
Tire radius: R	0.242m	Crown radius: CR	0.057m
Cornering stiffness: K_y	427.4N/deg	Camber stiffness: Q_y	17.77N/deg
Normalized K_y: C_y	42.74×10^{-2}/deg	Normalized Q_y: D_y	1.777×10^{-2}/deg
Pneumatic trail on slip angle: e_β	0.0136m	Pneumatic trail on camber angle: e_γ	-0.0267m

3. Steering Axis Specifications to be Determined

To uniquely define an axis in three-dimensional space, it is necessary to define 6 parameters for two points, or one point and one direction vector. In terms of determining the steering axis uniquely in the suspension design, this means determining four specification values other than the two specification values of the longitudinal position and tread of the front wheels.

The actual four independent parameters are caster angle (ξ), kingpin angle (ψ), caster trail (T_ξ) and kingpin offset (D_ψ) at ground level as shown in Figure 4. Alternatively, the tire radius (R) can be used to set T_{off}=T_ξ-$R\sin\xi$ and D_{off}=D_ψ-$R\sin\psi$ at the height of the wheel axis as independent values.

As a previous study with an automobile suspension in mind on the moment around the steering axis generated by the tire force on the road surface and the reaction force of the load, there are examples, that the authors discussed the steering pull phenomenon during braking on a rutted road focusing on the lateral movement of the load center on the ground [16,17], and the authors discussed the vehicle drift on slanted roads considering tire characteristics near neutral [18]. However, there is no example that discusses the steering torque characteristics of PMV.

Preprints (www.preprints.org) | NOT PEER-REVIEWED | Posted: 2 December 2022 doi:10.20944/preprints202212.0034.v1

In addition, as an example of previous study on PMVs that tilt inward when turning, the authors proposed a method to optimize steering torque characteristics on the pulled side [12]. There are also examples of motorcycles that discusses the directional stability using the camber angle [19] and that discusses the steering system torsional stiffness [20].

In order to uniquely derive the four specification values of the steering axis, it is necessary to determine the four target characteristic requirements for setting the steering axis. Based on the requirements of steering torque when a lateral force is applied to the tire on the road surface [12] and the requirement of straight-line stability when a longitudinal force is applied, we newly add the requirements for minimizing the disturbance around the steering axis due to the reaction force of vertical load from road surface. In order to satisfy the target number of requirements, the requirement when the vehicle is upright and the requirement when the vehicle is tilted are taken up as two independent target requirements [15].

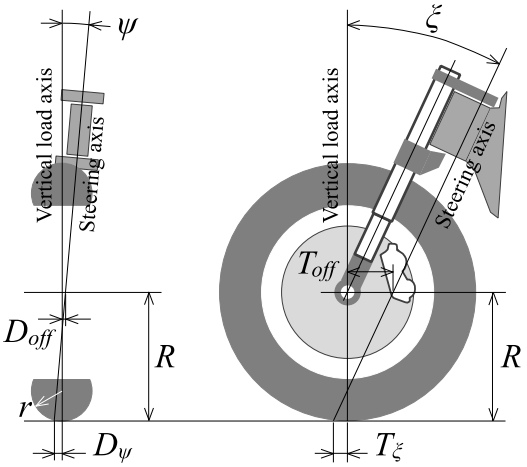

ht

Figure 4. Steering axis and four independent parameters.

4. Previous Studies Related to Steering Axis Geometry

4.1. Requirements for Caster Trail Considering Tire Lateral Force on the Road Surface [15]

According to the Reference [12], in case of PMVs that tilt inward when turning, the lateral force for turning is mostly obtained by the camber thrust and the moment in the pulled side is generated. In general, such torque characteristics are steered by the bar-handle of motorcycles, and there are no examples of steerability by the steering wheel like a car. For this reason, it seems difficult for the driver of the PMV who steers with the steering wheel to control the steering moment in the pulled side. Therefore, canceling this moment is the requirement for the caster trail (T_ε).

In addition, with PMVs that actively provide an inward tilt angle according to the steering angle and vehicle speed, an inadvertent large steering angle input on a low μ road induces an excessive inward inclination, creating the risk of overturning. In addition, counter steering during oversteering causes a dangerous outward tilt and induces trip over. In order to prevent these risks, it is necessary to avoid also the steering torque on the returning side due to excessive T_ε.

In the References [12] [13], as shown in Equation (2) and Figure 5a, 5b, it is proposed that the caster trail (T_ε) offsets the pneumatic trail (e_γ) caused by the camber angle, the additional torque proportional to the actual roll angle of the vehicle is added to the steering wheel in order to offset the hysteresis of the steering torque, and finally the additional torque proportional to the prospected lateral acceleration of the vehicle, proportional to the square of the vehicle speed and the steering wheel angle, is added to obtain an appropriate slope of the steering torque. The appropriate value of the added torque, which is proportional to the prospected lateral acceleration, should be determined

Preprints (www.preprints.org) | NOT PEER-REVIEWED | Posted: 2 December 2022 doi:10.20944/preprints202212.0034.v1

based on the human sense by actual vehicle driving, however this value is not related to this report. It is only concerned to offset the pneumatic trail (e_γ) due to the camber angle with the caster trail (T_ξ).

Therefore, based on the idea proposed in the References [12], we set T_ξ to be equal to the absolute value of the pneumatic trail (e_γ) due to the camber angle (γ) (T_ξ = 26.7mm) also in this report and proceed with the following study.

$$MT = \frac{\left(M_z + F_y(-e_\gamma)\right)}{r_s} + B_1 PLA + B_2 \varphi \quad (2)$$

MT: steering wheel torque
M_z: tire aligning moment
F_y: lateral force
e_γ: tire pneumatic trail on camber angle
r_s: steering ratio
B_1: aligning torque adjustment factor
PLA: provisional lateral acceleration
B_2: hysteresis adjustment factor
φ: tilt angle

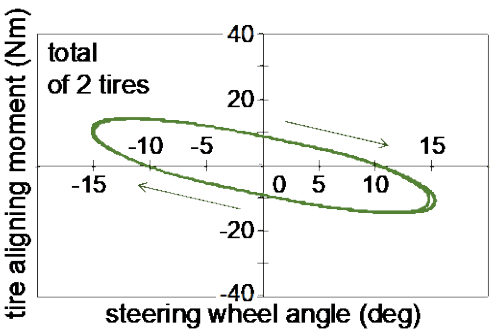

Figure 5a. Original tire aligning moment.

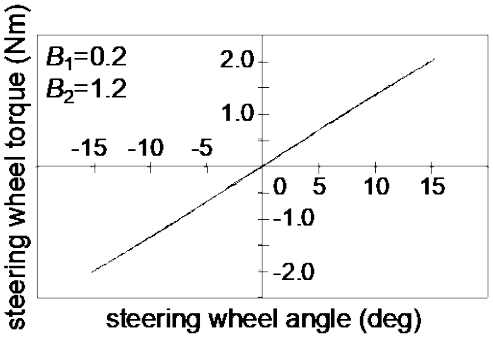

Figure 5b. Adjusted steering wheel torque.

4.2. Kingpin Offset Requirements Considering the Longitudinal Braking Force in the Contact Surface on Straight Running

As mentioned in the previous section, there is a proposal in the References [12] regarding lateral force input, however there is no example of a study that assumes PMV of the front two wheels for longitudinal force. Ideally, the vehicle should go straight during one-side braking even without the hand on steering wheel. For this purpose, the steering axis is placed outside the center of the ground point of the tire. As shown in Figure 6(b), the difference of toe-in moment due to the difference of braking force causes the front wheels steered to the smaller braking force side, and the yaw moment due to the lateral forces offsets the yaw moment disturbance due to the unbalance of braking forces [15].

This negative kingpin offset (D_ψ) is the requirement to keep straight running, as shown in the Equation (3) obtained by the simplified moment around the steering axis assumed nearly vertical due to the longitudinal force on the ground surface. This condition is shown in Figure 7. In automobiles, it is a constant value of about -21mm, and in motorcycles, it is always 0 mm. However, in case of PMVs with active inward tilting mechanism, an inward tilting angle that is proportional to the square of the vehicle speed and the steering angle is inevitably generated from Equation (1). Since a proportional lateral force by tire camber angle is generated, the requirement to run straight on one-side braking is the kingpin offset value, which is dependent on vehicle speed, as shown in Figure 7.

However, looking at the example of the kingpin offset value of a passenger car with a sufficient market experience, it is actually not a large negative value such as -21mm, but a modest value of -5mm at most [16,17]. This indicates that the requirements for straight running in the market for hands-free driving do not match the actual situation. As long as the driver holds the steering wheel, a large kingpin offset is not actually necessary, and

Preprints (www.preprints.org) | NOT PEER-REVIEWED | Posted: 2 December 2022 doi:10.20944/preprints202212.0034.v1

an excessive kingpin offset rather induces unpleasant rotational vibration of the steering wheel when ABS is activated. It is thought that this modest kingpin offset value was determined as a result. Since the market suitability of PMV is considered to be the same, regardless of the Equations (3) and Figures 7, this report sets the kingpin offset value at -5mm, following the example of passenger cars, and will proceed with further studies.

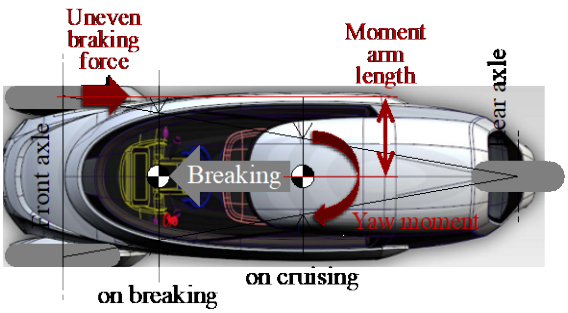

Figure 6a. Yaw moment on uneven braking force.

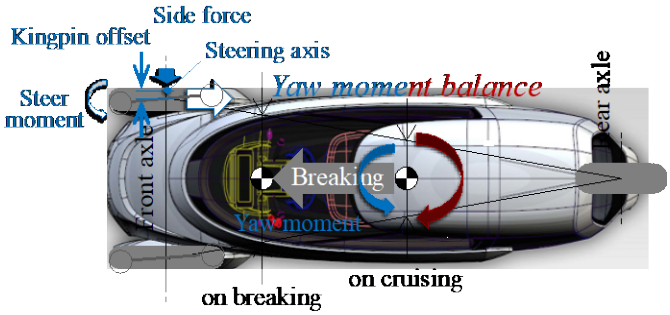

Figure 6b. Yaw moment balance on uneven braking force.

$$D_\psi \approx \frac{C_y Tr\left(T_\xi + e_\beta\right)}{2l_f\left(C_y + D_y \frac{v^2}{lg}\right)} \tag{3}$$

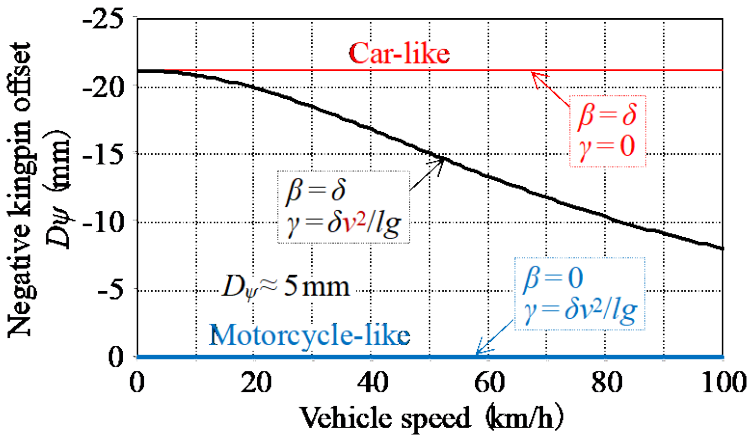

Figure 7. D_ψ to minimize yaw moment disturbance by one-side braking.

5. A Method to Minimize Steering Disturbance Caused by Uneven Road Surface for Personal Mobility Vehicle (PMV) with Inward Tilting Mechanism [15]

Of the four independent parameters described in Chapter 3.: caster angle (ξ), kingpin angle (ψ), caster trail (T_ξ), and kingpin offset at ground level (D_ψ), caster trail (T_ξ) and kingpin offset (D_ψ) have already been assumed according to Chapter 4., therefore in this chapter the caster angle (ξ) and kingpin angle (ψ) are derived from the two target characteristics of minimizing steering disturbance due to the reaction force against vertical load when standing upright, and of maintaining zero steering disturbance due to the reaction force against vertical load even if the tire contact point moves laterally when the vehicle is tilted inward.

5.1. Minimization of Steering Disturbance due to Reaction Force Against Vertical Load when Standing Upright

As shown in Figure 8, if the point on the ground on the steering axis is $P_1(x_1, y_1, 0)$, the other point is $P_2(x_2, y_2, z_2)$, and $|P_1\text{-}P_2|=1$, the four parameters ξ, ψ, T_ξ, and D_ψ are represented by four coordinate values x_1, y_1, x_2, and y_2 as follows.

$$tan\xi = (x_2 - x_1)/z_2 \quad \xi: Caster\ angle$$

Preprints (www.preprints.org) | NOT PEER-REVIEWED | Posted: 2 December 2022 doi:10.20944/preprints202212.0034.v1

$$tan\psi = (y_2 - y_1)z_2 \quad \psi: \text{Kingpin angle}$$
$$T_\xi = -x_1 \quad T_\xi: Caster\ trail$$
$$D_\psi = -y_1 \quad D_\psi: Kingpin\ offset$$
$$z_2^2 = 1 - (x_2 - x_1)^2 - (y_2 - y_1)^2$$

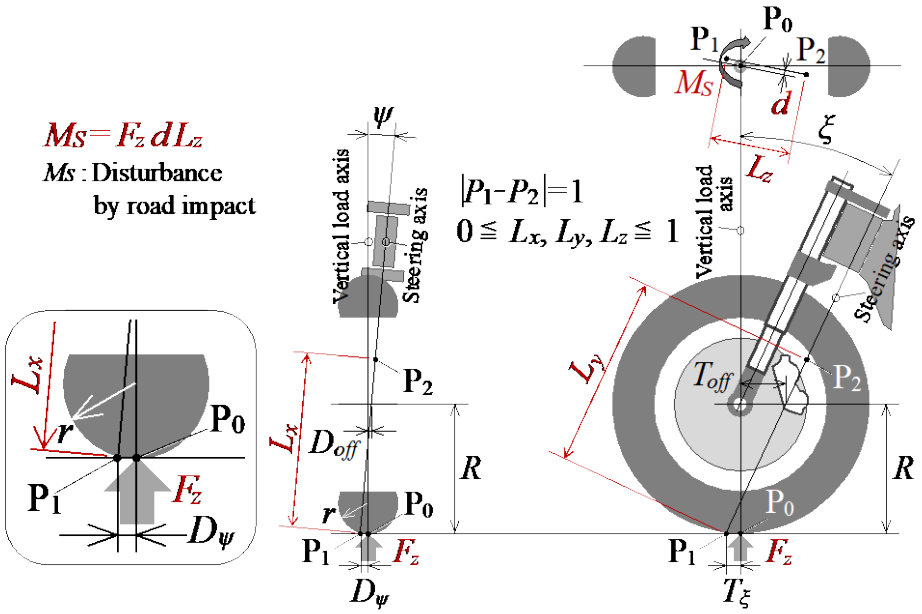

Figure 8. Steering moment disturbance (M_S) by road impact (F_z).

Here, the projection length L_z to the x-y plane, the projection length L_x to the y-z plane, and the projection length L_y to the z-x plane of the line segment P_1-P_2 are as follows.

$$\begin{aligned} L_x^2 &= (y_2 - y_1)^2 + z_2^2 = 1 - (x_2 - x_1)^2 \\ L_y^2 &= (x_2 - x_1)^2 + z_2^2 = 1 - (y_2 - y_1)^2 \\ L_z^2 &= (x_2 - x_1)^2 + (y_2 - y_1)^2 \end{aligned} \tag{4}$$

From $|P_1\text{-}P_2|=1$, L_x is the efficiency of the moment around the steering axis created by the vertical force by the longitudinal force, L_y is by the lateral force, and L_z is by the efficiency. L_x, L_y and L_z are also represented by four coordinate values x_1, y_1, x_2, and y_2.

The reaction force axis is defined by the vertical axis passing through the center of the ground point $P_0(x_0, y_0, 0)$ in Figure 8. This reaction force axis and the steering axis are generally in a skew position. Since the reaction force axis is vertical, the distance between the two axes is equal to the distance d between the point P_0 and the steering axis P_1-P_2 in planar view as shown in Figure 8.

If P_1-P_2 in planar view is set to $ax+by+c=0$,

$$\begin{aligned} a &= y_2 - y_1 \\ b &= -(x_2 - x_1) \\ c &= x_2 y_1 - x_1 y_2 \end{aligned}$$

d is expressed as;

$$d^2 = (ax_0 + by_0 + c)^2/(a^2 + b^2) \tag{4*}$$

Also, Equation (4) can be transformed into;

$$L_z^2 = a^2 + b^2 \tag{4**}$$

Here, the moment M_S around the steering axis due to the reaction force against vertical load F_z is expressed by Equation (5) as the product of these.

$$M_S = F_z dL_z \tag{5}$$

Preprints (www.preprints.org) | NOT PEER-REVIEWED | Posted: 2 December 2022 doi:10.20944/preprints202212.0034.v1

When the vehicle is upright, the coordinates of the center of the ground point P_0 are (0, 0, 0) and d is $d^2=c^2/(a^2+b^2)$. By substituting Equations (4*) and (4**) into Equation (5), the moment around the steering axis (M_S) becomes Equation (5*).

$$M_S = F_z d L_z = F_z C = F_z (x_2 y_1 - x_1 y_2)^{1/2} \quad (5^*)$$

The condition of $M_S = 0$ is shown in Equation (6) by modifying $c = x_2y_1\text{-}x_1y_2 = 0$, and Figure 9 is obtained by substituting $T_\xi = 26.7$mm and $D_\psi = 5$mm.

$$\frac{y_1}{x_1} = \frac{y_2}{x_2} = \frac{D_\psi}{T_\xi} = \frac{tan\psi}{tan\xi} \quad (6)$$

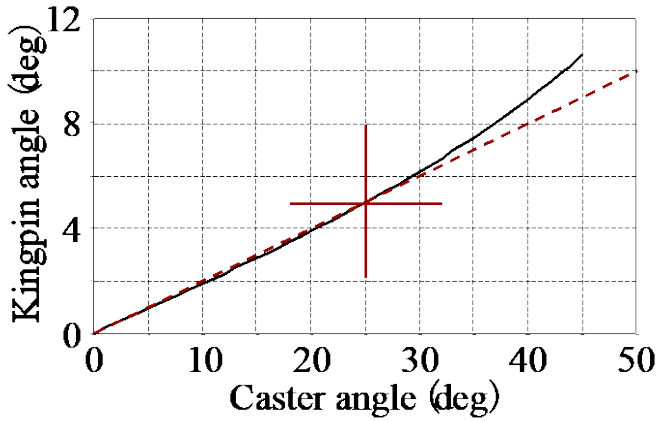

Figure 9. Steering axis to minimize M_S by F_z on zero roll condition.

Expressing d=0 graphically, as shown in Figure 10, it is a special state where the reaction force axis and the steering axis intersect at the point P_h. If the coordinates of P_h are (0, 0, h), h is expressed by Equation (7).

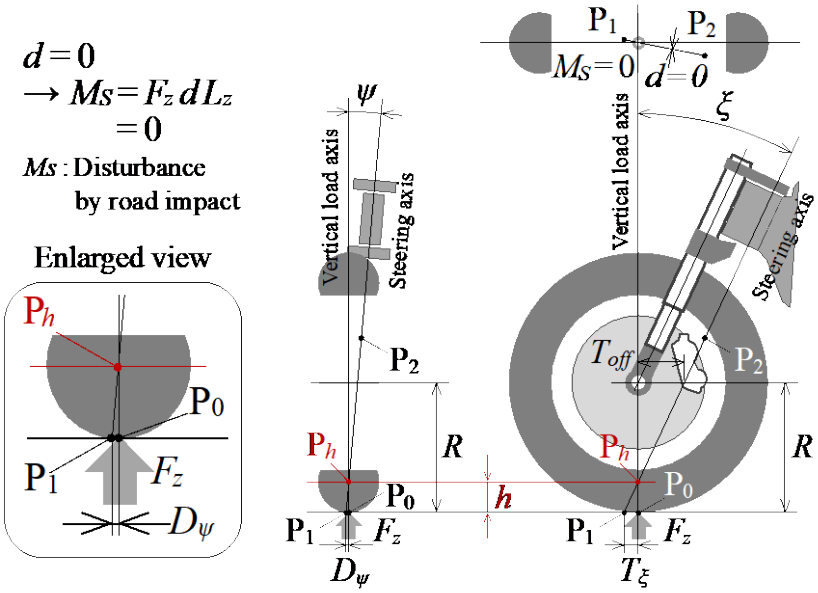

Figure 10. Steering axis to minimize M_S by F_z on upright condition.

$$h = \frac{T_\xi}{tan\xi} = \frac{D_\psi}{tan\psi} \quad (7)$$

5.2. Maintaining Zero Steering Disturbance due to the Reaction Force Against Vertical Load even if the Tire Contact Point Moves Laterally when the Vehicle is Tilted Inward

Preprints (www.preprints.org) | NOT PEER-REVIEWED | Posted: 2 December 2022 doi:10.20944/preprints202212.0034.v1

Figure 11 shows the lateral movement of the tire contact point, and the reaction force when the tire is tilted inward, with the crown radius (r) enlarged for clarity. When the vehicle body tilts by an angle φ, the steering axis rotates with the tires. Points P_0, P_1, P_2 move to P_0^*, P_1^*, P_2^*.

$$P_0(0,0,0),\ \ P_1(x_1,y_1,0),\ \ P_2(x_2,y_2,z_2)$$
$$x_1 = -T_\xi,\quad x_2 = x_1 + L_y sin\xi$$
$$y_1 = -D_\psi, y_2 = y_1 + L_x sin\psi$$
$$z_2 = L_x cos\psi = L_y cos\xi$$
$$P_0^*(0, y_0^*, z_0^*) = \left(0, r(\varphi - sin\varphi), r(1 - cos\varphi)\right)$$
$$P_1^*(x_1, y_1^*, z_1^*) = \left(x_1, y_0^* - D_\psi cos\varphi, z_0^* + D_\psi sin\varphi\right)$$
$$P_2^*(x_2, y_2^*, z_2^*) = \left(x_2, y_1^* - L_x sin(\varphi + \psi), z_1^* + L_x cos(\varphi + \psi)\right)$$

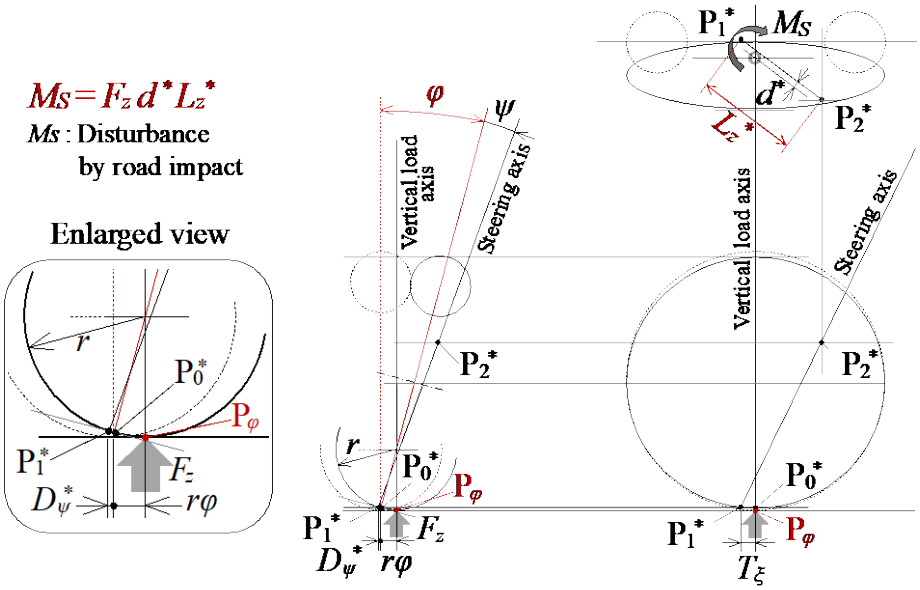

Figure 11. Steering axis on tilted condition.

As shown in Figure 11, the tire contact point P_φ moves from P_0 to the inner side of the vehicle by $r\varphi$, and becomes $P_\varphi(0, y_\varphi, 0)=(0, r\varphi, 0)$. Assuming that the steering axis P_1^*-P_2^* during tilt is $a^*x+b^*y+c^*=0$,

$$a^* = y_2^* - y_1^*$$
$$b^* = b = -(x_2 - x_1)$$
$$c^* = x_2 y_1^* - x_1 y_2^*$$

d^* is expressed as

$$d^{*2} = (br\varphi + c^*)^2/(a^{*2} + b^2)$$

Also, the projection length L_z^* of the line segment P_1^*-P_2^* onto the x-y plane is as follow.

$$L_z^{*2} = (x_2 - x_1)^2 + (y_2^* - y_1^*)^2 = a^{*2} + b^2$$

Here, the condition for $M_s=F_z d^* L_z^*=F_z(br\varphi+c^*)=0$ is $br\varphi+c^*=0$.

For the sake of simplicity, if we graphically consider the state where the reaction force axis and the steering axis intersect, the coordinates of the intersection point P_h^* are $(0, r\varphi, h)$, where h corresponds to r shown as Figure 12. Equation (8) is obtained regardless of φ.

Preprints (www.preprints.org) | NOT PEER-REVIEWED | Posted: 2 December 2022 doi:10.20944/preprints202212.0034.v1

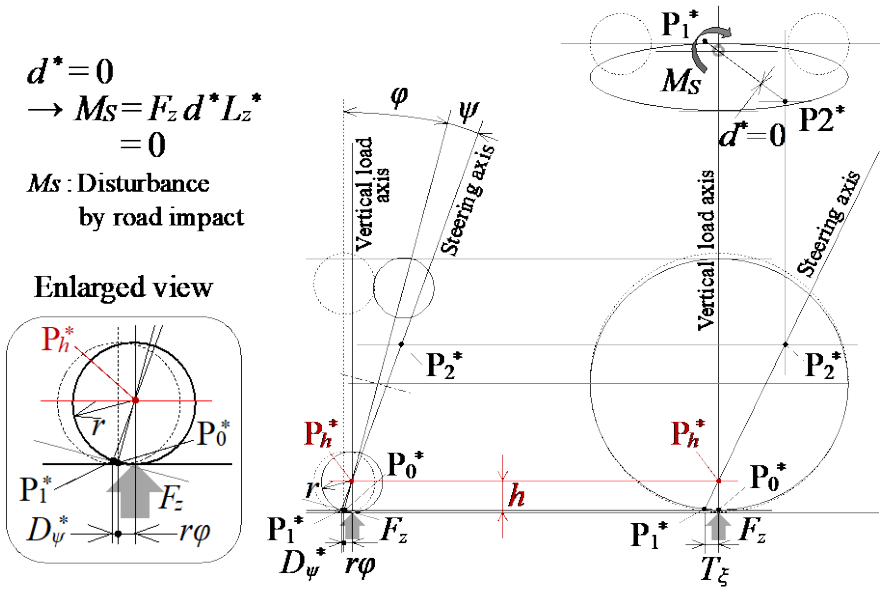

Figure 12. Steering axis to minimize M_s by F_z on tilted condition.

$$r = h = \frac{T_\xi}{tan\xi} = \frac{D_\psi}{tan\psi} \tag{8}$$

5.3. Specification Setting Procedure for Minimizing Steering Disturbance due to the Reaction Force Against Vertical Load

When planning a vehicle, the tire size is determined according to its load capacity based on vehicle mass and maximum speed requirements. If the size is too small, there is concern that the load capacity will be insufficient. If the size is too large, the unsprung road trackability deteriorates and the grip of the tire becomes unstable. In other words, the appropriate tire size is almost uniquely determined according to the vehicle size, and the crown radius (r) is also almost uniquely determined.

Figure 13 shows the procedure for setting the steering axis specifications when the crown radius (r) is determined, as a summary of the method for minimizing the disturbance around the steering axis due to the reaction force against vertical load. Assuming T_ξ=0.0267m from Section 4.1. and D_ψ=0.005m from Section 4.2.,

(1) Caster angle (ξ) = 25deg is obtained from r = 0.057m in order to maintain the d value during tilt.

(2) In order to set d=0 when standing upright, the kingpin angle (ψ)=5deg can be obtained from ξ=25deg.

Using the tire radius (R) = 0.2424m, the offset of the steering axis at the height of the wheel axis is as follows.

$$T_{off} = T_\xi - Rsin\xi = 0.0267 - 0.2424sin(25deg) = -0.0757m$$
$$D_{off} = D_\psi - Rsin\psi = 0.005 - 0.2424sin(5deg) = -0.0161m$$

Preprints (www.preprints.org) | NOT PEER-REVIEWED | Posted: 2 December 2022 doi:10.20944/preprints202212.0034.v1

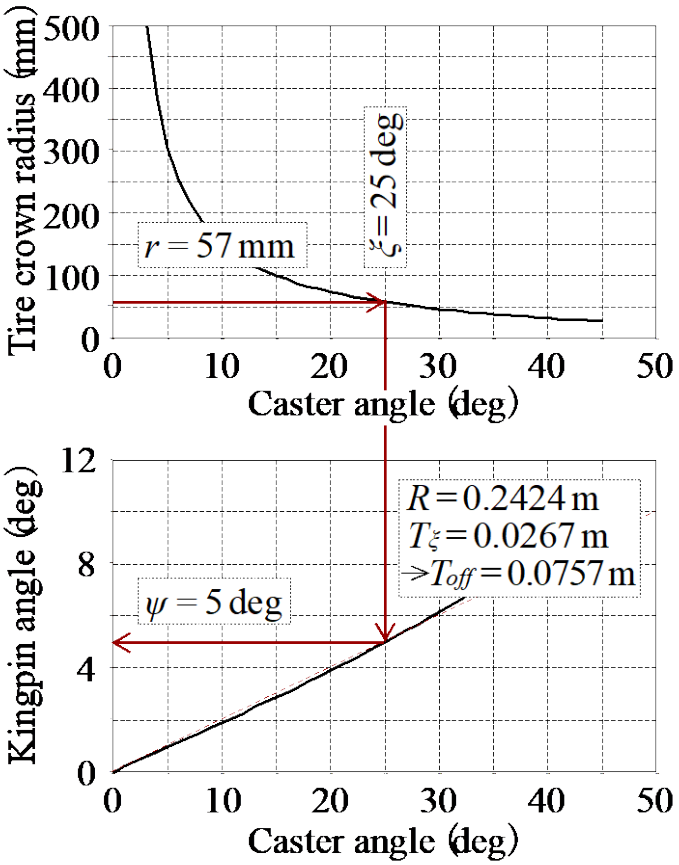

Figure 13. Procedure to set the steering specifications.

6. Vehicle Stability During Disturbance Caused by Uneven Road Surface in the Market, Using the Method to Minimize Steering Disturbance

As an application of maintaining zero steering disturbance due to the reaction force against vertical load even if the tire contact point moves laterally when the vehicle is tilted inward, first consider the state of maintaining straight running on a slanted road surface with a transverse slope. Next, the ability to maintain straight running on rutted roads, which are often encountered in the market along with slanted roads, is also considered.

6.1. Lateral Force Balance on Slanted Road

In a vehicle without an inward tilting mechanism, the lateral force that prevents the vehicle from sliding down along the road surface is generated by the slip angle of all wheels caused by the vehicle slip angle, as shown in Figure 14. Assuming that the lateral transfer of vertical load between both wheels and the slip angle, due to slant are sufficiently small, and that there is no front wheel steered angle, the lateral force balance is expressed by Equation (9a), and the required slip angle (β) is obtained by Equation (9b). In order to generate this slip angle (β), a yaw angle of angle (β) is generated in the vehicle body. The yaw moment balance is expressed by Equation (10a), but this equation is nothing more than the indication of the vehicle's center of gravity (G.C.) position (Equation (10b)). In the transition section from a road surface without slant to a road surface with slant angle (φ), dynamic response is affected by yaw inertia (I_z) and roll inertia (I_x). However, it transitions relatively quickly to the balanced state above, under the condition both β and φ are small.

$$\beta_r = \beta_{fL} = \beta_{fR} = \beta \qquad F_{y\beta r} \approx K_{yr}\beta = C_y F_{zr}\beta$$
$$F_{y\beta fL} \approx K_{yfL}\beta = C_y F_{zfL}\beta \qquad F_{y\beta fR} \approx K_{yfR}\beta = C_y F_{zfR}\beta$$
$$mgsin\varphi = F_y = F_{y\beta r} + F_{y\beta fL} + F_{y\beta fR} = C_y\beta\left(F_{zr} + F_{zfL} + F_{zfR}\right) = mgC_y\beta \quad (9a)$$
$$\beta = sin\varphi/C_y \approx \varphi/C_y \quad (9b)$$

Preprints (www.preprints.org) | NOT PEER-REVIEWED | Posted: 2 December 2022 doi:10.20944/preprints202212.0034.v1

$$F_{y\beta r} l_r = \left(F_{y\beta fL} + F_{y\beta fR}\right) l_f$$
$$C_y \beta F_{zr} l_r = C_y \beta \left(F_{zfL} + F_{zfR}\right) l_f \quad (10a)$$
$$F_{zr} / \left(F_{zfL} + F_{zfR}\right) = l_f / l_r \quad (10b)$$

x: longitudinal direction y: lateral direction v: vehicle speed
m: vehicle mass g: gravitational acceleration
l: wheel base Tr: front tread G.C.: gravity center
l_f: front distance from G.C. l_r: rear distance from G.C.
φ: slant angle (≈tilt angle) GCH: gravity center height
K_y: cornering stiffness C_y: normalized cornering stiffness

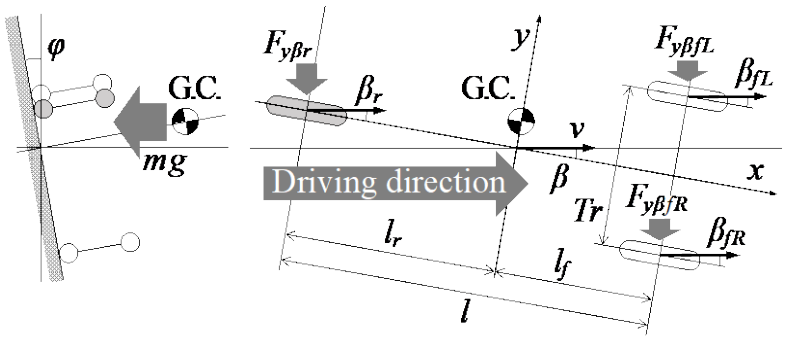

Figure 14. Straight running on slanted road without inward tilting (Car like).

Next, consider a vehicle with an inward tilting mechanism. According to the Reference [14], when the inward tilt angle of the motorcycle is just balanced with the roll moment during turning (Equation (11)), the lateral force due to the tire camber angle that accompanies the inward tilt is generally set to almost the value that it just balances the centrifugal force. This is not limited to the tires assumed in this report. As shown in Figure 15, when a PMV with an inward tilting mechanism remains upright on a road surface with a slant angle, this relationship means that the lateral force generated by the camber angle of the tires prevents the vehicle from slide down along the road surface. Therefore, the PMV keeps to run straight. At this time, there is no lateral transfer of vertical load due to the slant, no tire slip angle is required unlike a vehicle without an inward tilting mechanism, and no yaw angle is required for the vehicle body.

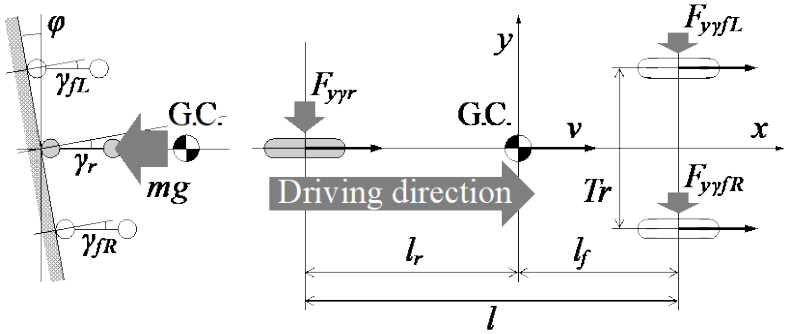

Figure 15. Straight running on slanted road with inward tilting (MC like).

$$\varphi = tan^{-1}(v^2/\rho) \quad (11)$$
$$\gamma_r = \gamma_{fL} = \gamma_{fR} = \gamma = \varphi \qquad F_{y\gamma r} \approx Q_{yr}\gamma = D_y F_{zr}\gamma$$
$$F_{y\gamma fL} \approx Q_{yfL}\gamma = D_y F_{zfL}\gamma \qquad F_{y\gamma fR} \approx Q_{yfR}\gamma = D_y F_{zfR}\gamma$$
$$mgsin\varphi = F_y = F_{y\gamma r} + F_{y\gamma fL} + F_{y\gamma fR} = D_y\gamma\left(F_{zr} + F_{zfL} + F_{zfR}\right) = mgD_y\gamma \quad (12a)$$
$$\gamma = \varphi \approx sin\varphi / D_y \qquad D_y \approx sin\varphi/\varphi \quad (12b)$$
$$F_{y\gamma r} l_r = \left(F_{y\gamma fL} + F_{y\gamma fR}\right) l_f$$
$$D_y\gamma F_{zr} l_r = D_y\gamma\left(F_{zfL} + F_{zfR}\right) l_f \quad (13)$$

Q_y: camber stiffness D_y: normalized camber stiffness

Preprints (www.preprints.org) | NOT PEER-REVIEWED | Posted: 2 December 2022 doi:10.20944/preprints202212.0034.v1

Figure 15 simply shows the balance when traveling straight on a slanted road, ignoring the lateral movement of the tire contact point due to the camber angle (γ) against road surface. The lateral force balance is expressed by Equation (12a), and the normalized camber stiffness (D_y) required to realize the state shown in Figure 3 is obtained by Equation (12b). The balance of the yaw moment is expressed by equation (13), but this equation is nothing more than the indication of the vehicle's center of gravity (G.C.) position (Equation (10b)). This relationship is equivalent to the balance state of a motorcycle running straight on a slanted road.

Figure 16 shows the details of one wheel in Figure 15 as viewed from the rear, and considers the lateral movement of the tire contact point due to the camber angle against road surface. The amount of lateral movement is expressed as $CR\sin\varphi$ using the tire crown radius. In order to offset the turnover moment in the roll direction, the vehicle leans slightly to the mountain side. Therefore, the camber angle (γ) against road surface is slightly larger than the slant angle (φ) by $\Delta\varphi$ as shown in Equation (14).

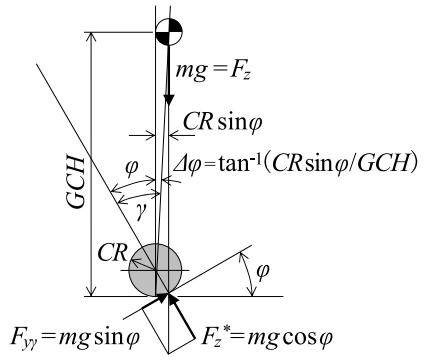

Figure 16. Lateral movement of the grounding point on a slant road.

$$\gamma = \varphi + \Delta\varphi = \varphi + tan^{-1}(CRsin\varphi/GCH) \quad (14)$$

$$F_{y\gamma} = (\gamma + \Delta\gamma)D_y F_z^* = (\varphi + \Delta\varphi)D_y mgcos\varphi = mgsin\varphi \quad (15a)$$

$$D_y = mgsin\varphi/\big((\varphi + \Delta\varphi)mgcos\varphi\big) = tan\varphi/(\varphi + \Delta\varphi) \quad (15b)$$

Equation (15a) must hold in order to balance the lateral forces at zero slip angle (β). By modifying Equation (15a), the normalized camber stiffness (D_y) required to maintain straight running on a slant road is obtained by Equation (15b). Using the same tire crown radius (CR=57mm) as in Reference (15), the necessary normalized camber stiffness (D_y) for the slant angle (φ) is almost constant as shown in Figure 17. When φ=10deg, D_y =1.522×10-2/deg, and this value is almost equal to the value of D_y required for turning only with camber stiffness (Q_y), which is obtained in Reference [14]. In other words, for a PMV that tilts inward when turning, by giving appropriate tire characteristics, it is possible to achieve both turning characteristics that do not produce a slip angle (β) during turns and straight running ability on slant roads.

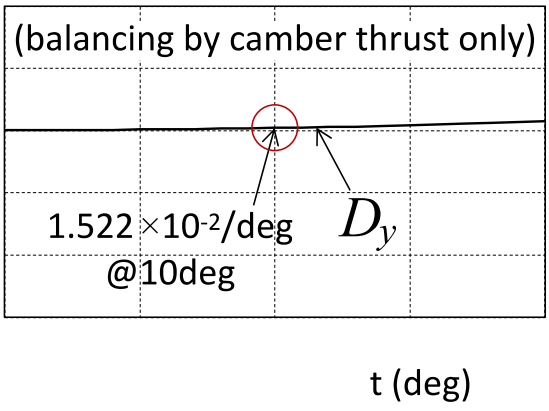

Figure 17. Normalized camber stiffness to cancel the road slant.

Preprints (www.preprints.org) | NOT PEER-REVIEWED | Posted: 2 December 2022 doi:10.20944/preprints202212.0034.v1

6.2. Straight Running Stability on Slanted Road

In order for the vehicle to maintain straight running without being affected by road surface disturbances, as discussed in References [16-18], it is required that lateral force is balanced without steering operation, yaw moment does not occur and steering moment also does not occur. Figure 18 shows the details of the caster trail changes in the side view due to the movement of the tire contact point, in addition to the details of the rear view of the tire. Since $\Delta\varphi$ is small, the tire is assumed circular in side view. The effective caster trail (T_ξ^*) is slightly smaller than the caster trail (T_ξ) as a suspension specification because the tire contact point is slightly higher than the original position due to lateral movement of tire contact point. Expressed as an equation, it is smaller by $CR(1\text{-}\cos\varphi)\sin\xi$ as shown in Equation (16), however, the difference is very small that it can be ignored compared to T_ξ as shown in Figure 19.

The moment around the steering axis consists of the sum of the moments by vertical load against road surface and lateral force along with road surface. The moment by the vertical load (F_z^*) against road surface is equal to the moment around the steering axis when tilts inward due to the reaction force of the vertical load (F_z) in Section 5.2. This is already zero, since the steering axis is followed the specification that satisfies the minimization requirement in Section 5.2. The steering moment (M_z^*) around the steering axis due to the lateral force is given by Equation (17). Since $CR(1\text{-}\cos\varphi)\sin\xi$ is negligibly small compared to T_ξ, M_z^* is effectively zero. In other words, as long as the concept of steering axis setting shown in Section 5.3. is followed, when running on a transverse slant road, the steering moment is not generated at the same time as the lateral force balance and the yaw moment balance.

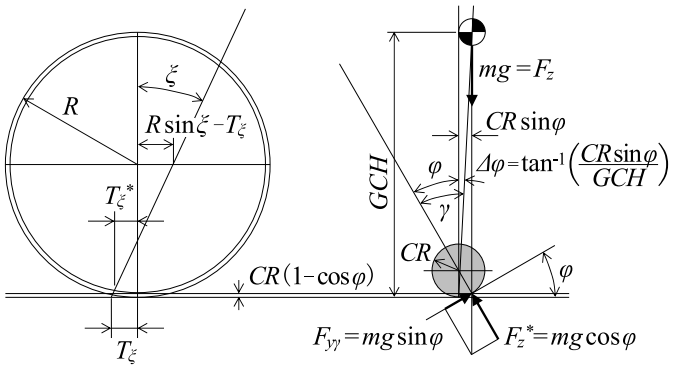

Figure 18. Steering geometry on a slant road.

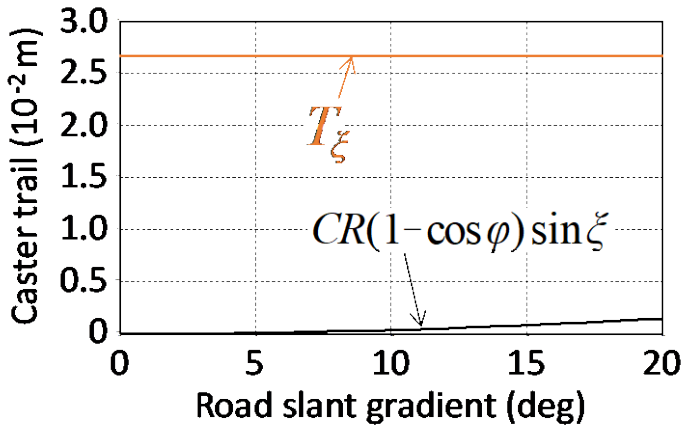

Figure 19. Reduced caster trail on a slant road.

$$T_\xi^* = \big(R - CR(1-cos\varphi)\big)sin\xi - \big(Rsin\xi - T_\xi\big) = T_\xi - CR(1-cos\varphi)sin\xi \quad (16)$$

$$M_z^* = F_{y\gamma}\big(e_\gamma + T_\xi^*\big)cos\xi cos\psi = mgsin\varphi cos\xi cos\psi\big(e_\gamma + T_\xi - CR(1-cos\varphi)sin\xi\big) \quad (17)$$

Preprints (www.preprints.org) | NOT PEER-REVIEWED | Posted: 2 December 2022 doi:10.20944/preprints202212.0034.v1

Unlike a vehicle without an inward tilting mechanism, the vehicle body remains upright, therefore only the unsprung part is involved in the dynamic response in the transition section, and the vehicle can move to the balanced state on the transverse slant part more quickly than a vehicle without an inward tilting mechanism. However, the dynamic slant angle changes produce the significant vertical load change. As described in Chapter 5., if no moment is generated around the steering axis regardless of vertical load fluctuations, disturbance is minimized even in the slant angle transition section. Therefore, it can be said that the straight running ability of PMVs is extremely good.

6.3. Straight Running Stability on Rutted Road

In the actual market, the transvers slant of the road surface (Figure 20(a)) is a typical disturbance, but the rut is also a typical disturbance [16,17]. As shown in Figure 20(b) to (d), in the case of ruts, unlike the case of slant, there is no particular difference in the height of both wheels. As for the ruts, it is necessary to divide them into several cases, such as the difference in tread and the ruts formed by the twin tires of a large vehicle. When a PMV with a narrow tread runs on a rutted road formed by a passenger car or a large vehicle, various inconsistent situations can be assumed, such as the tread width of the PMV is close to the tread width of the rut and both wheels are positioned on the same side of the rut as shown in Figure 20(b), such as the tread width of the PMV is narrower than the tread width of the ruts of a passenger car and only one wheel is affected by the ruts as shown in Figure 20(c), and such as the tread width of the PMV is fairly narrow and both wheels are positioned on symmetrical slopes on the even narrower ruts formed by the twin tires of large vehicles as shown in Figure 20(d).

In order to maintain straight running without being disturbed by the transvers slope of the road surface in any of these inconsistent situations, the lateral force generated by the transvers slope of the road surface and the moment around the steering axis should not be canceled between the left and right wheels and lateral force and the moment must be avoided independently in each wheel. As mentioned in the discussion of straight running ability on slanted roads, if each of the both wheels independently minimize disturbances in terms of both the lateral force on slanted roads and the moment around the steering axis, straight running ability is maintained even under all ruts condition.

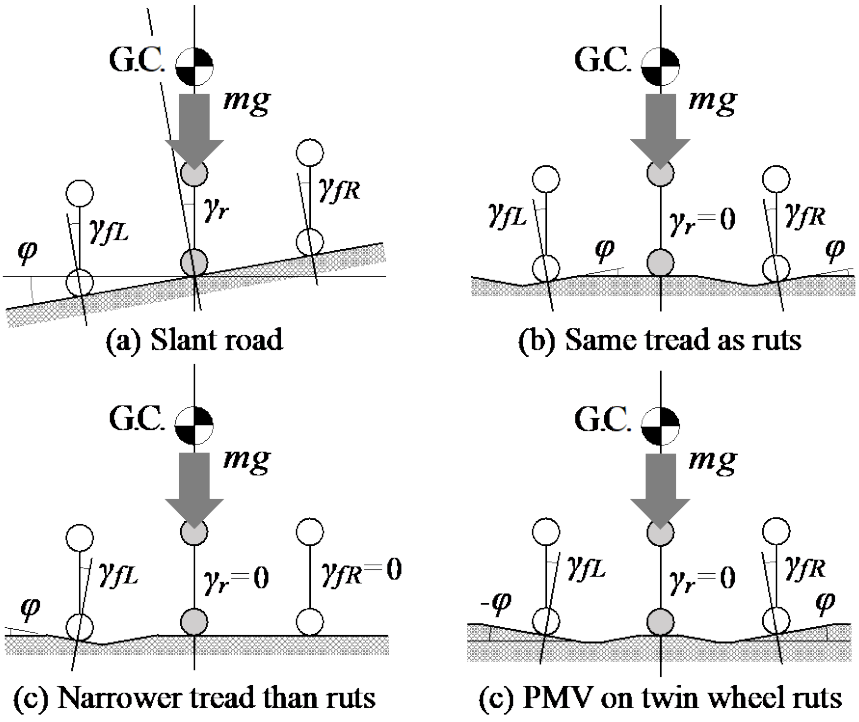

Figure 20. PMV running on a slant road and typical rutted roads.

 doi:10.20944/preprints202212.0034.v1

7. Conclusions

In this paper, we studied the stability of the vehicle when external disturbances are input from the road surface, such as sudden changes in reaction force against vertical load (impact from the road surface) due to road surface unevenness, and such as the transvers inclination of road surface due to slant and ruts. Then we derived the design requirements for the steering axis of PMVs to maintain straight running ability against such disturbances.

As the future works, we authors will proceed to study dynamic vehicle behavior based on this consideration of static balance. At first the direct verification of this mechanical consideration will be proceeded using a multibody dynamics (MBD) model, prior to the driving tests on actual vehicles. We will continue our activities to realize an ultra-compact PMV by making use of the knowledge obtained in this study.

Author Contributions: Conceptualization, T.H.; methodology, T.H.; software, T.H. and T.K.; validation, T.H.; formal analysis, T.H.; investigation, T.H. and T.K.; resources, T.H. and T.K.; data curation, T.H.; writing—original draft preparation, T.H.; writing—review and editing, T.H.; visualization, T.H.; supervision, T.H.; project administration, T.H.; funding acquisition, T.H. and T.K. All authors have read and agreed to the published version of the manuscript.

Funding: This research received no external funding.

Data Availability Statement: Not applicable.

Conflicts of Interest: The authors declare no conflict of interest.

References

1. Haraguchi, T. 4. Personal Mobility Vehicle. *Mobility Service, Mobility Innovation Series*; Corona Publishing Co., Ltd.: Tokyo, Japan, **2020**; Volume 1, pp. 92-123, ISBN 978-4-339-02771-6.
2. Haraguchi, T. Prospects for Future Personal Mobility (PMV) from a Historical Background. *Automotive Technology*; Technical Information Institute Co., Ltd.: Tokyo, Japan, **2020**; Volume 8-2, pp. 63-67, ISSN2432-5694.
3. Kaneko, T; Kageyama, I.; Haraguchi, T.; Kuriyagawa, Y. A Study on the Harmonization of a Personal Mobility Vehicle with a Lean Mechanism in Road Traffic (1st Report): Micro-Scale Traffic Flow Simulation in Consideration of Mutual Interference of Driver Risk Feeling. In Proceedings of JSAE Annual Meeting, Yokohama, Japan, May **2016**, No.55-16, pp.1350-1354, 20165255.
4. Haraguchi, T.; Kaneko, T.; Kageyama, I.; Kuriyagawa, Y.; Kobayashi, M. Study of Tilting Type Personal Mobility Vehicle by the Immersive Driving Simulator with Five Large Screens. *Trans. JSAE* **2017**, Vol.48-3, pp. 693-698, 20174447.
5. Haraguchi, T.; Kaneko, T.; Kageyama, I. Market Acceptability Study on Energy Balance of Personal Mobility Vehicle (PMV) with Active Tilting Mechanism. In Proceedings of JSAE Annual Meeting, Yokohama, Japan, May **2019**, No.59-19, pp.1-6, 20195284.
6. Haraguchi, T.; Kageyama, I.; Kaneko, T. Study of Personal Mobility Vehicle (PMV) with Active Inward Tilting Mechanism on Obstacle Avoidance and Energy Efficiency. *Applied Sciences*; Multidisciplinary Digital Publishing Institute (MDPI) **2019**, Vol.9, 4737, DOI:10.3390/app9224737.
7. Haraguchi, T.; Kaneko, T.; Kageyama, I.; Kobayashi, M.; Murayama, T. Obstacle Avoidance Maneuver of Personal Mobility Vehicles with Lean Mechanism: Comparison between Front and Rear Wheel Steering. In Proceedings of JSAE Annual Meeting, Yokohama, Japan, May **2017**, No.18-17, pp.494-499, 20175092.
8. Kaneko, T; Kageyama, I.; Haraguchi, T. Dynamic Rollover Characteristics of Personal Mobility Vehicles with Lean Mechanism. In Proceedings of JSAE Annual Meeting, Osaka, Japan, October **2017**, No.163-17, pp.1392-1397, 20176258.
9. Haraguchi, T.; Kaneko, T.; Kageyama, I. Study on Steering Response of Personal Mobility Vehicle (PMV) by Comparison of PMV with Passenger Cars and Motorcycles on the Obstacle Avoidance Performance. In Proceedings of JSAE Annual Meeting, Nagoya, Japan, October **2018**, No.113-18, pp.1-6, 20186058.
10. Haraguchi, T.; Kageyama, I.; Kaneko, T. Inner Wheel Lifting Characteristics of Tilting Type Personal Mobility Vehicle by Sudden Steering Input. *Trans. JSAE* **2019**, Vol.50-1, pp. 96-101, 20194038.
11. Kaneko, T; Kageyama, I.; Haraguchi, T. A Study on Characteristics of the Vehicle Response by Abrupt Operation and an Improvement Method for Personal Mobility Vehicle with Leaning Mechanism. *Trans. JSAE* **2019**, Vol.50-3, pp. 796-801, 20194345.
12. Haraguchi, T.; Kaneko, T.; Kageyama, I. Steering Torque Characteristics of Personal Mobility Vehicle (PMV) with Inward Tilting Mechanism. *Trans. JSAE* **2020**, Vol.51-5, pp. 931-937, 20204471.
13. Haraguchi, T.; Kaneko, T.; Kageyama, I. Steering Torque Hysteresis of Personal Mobility Vehicle (PMV) with Inward Tilting Mechanism. *Trans. JSAE* **2021**, Vol.52-5, pp. 987-993, 20214638.
14. Haraguchi, T.; Kaneko, T.; Kageyama, I. A Study of Steer Characteristics of Personal Mobility Vehicle (PMV) with Inward Tilting Mechanism. *Trans. JSAE* **2022**, Vol.53-1, pp. 58-64, 20224033.
15. Haraguchi, T.; Kaneko, T.; Kageyama, I. A Method to Minimize Steering Disturbance Caused by Vertical Load Reaction Force of Personal Mobility Vehicle (PMV) with Inward Tilting Mechanism. *Trans. JSAE* **2021**, Vol.52-2, pp. 462-468, 20214197.
16. Kato, K.; Haraguchi, T. Improvement on Steering Pull during Braking on Wheel Tracks. *Journal of Society of Automotive Engineers of Japan* **1994**, Vol.48-12, pp.66-71, NDL-ID 3903809.
17. Kato, K.; Haraguchi, T. Improvement on steering pull during braking on rutted road. *JSAE Review* **1996**, Vol.17-1, pp71-74.
18. Yamada, Y.; Haraguchi, T. Analysis of Vehicle Drift on the Cant Road. *Journal of Society of Automotive Engineers of Japan* **1995**, Vol.49-12, pp.65-70, NDL-ID 3638366.
19. Kageyama, I.; Makita, M.; Kuriyagawa, Y. Fundamental Study on Directional Control of PMV Using Karge Camber Angle Control. *Trans. JSAE* **2015**, Vol.46-5, pp. 919-924, 20154568.
20. Kageyama, I.; Kuriyagawa, Y.; Haraguchi, T.; Kobayashi, Y. Two-wheeled Vehicle Characteristics on Steady State Turning Considering Equivalent Compliance. *Trans. JSAE* **2019**, Vol.50-5, pp. 1402-1408, 20194696.